Spring 4-2013

Thickness-Shear Vibration Of A Rectangular Quartz Plate With Partial Electrodes

Huijing He
University of Nebraska-Lincoln, he.hui.jing@hotmail.com

Jiashi Yang
University of Nebraska-Lincoln, jyang1@unl.edu

John A. Kosinski
Monmouth University

Ji Wang
Ningbo University, wangji@nbu.edu.cn

Acta Mechanica Solida Sinica, Vol. 26, No. 2, April, 2013 ISSN 0894-9166
Published by AMSS Press, Wuhan, China

THICKNESS-SHEAR VIBRATION OF A RECTANGULAR QUARTZ PLATE WITH PARTIAL ELECTRODES**

Huijing He[1] **Jiashi Yang**[1] **John A. Kosinski**[2] **Ji Wang**[3*]

([1] *Department of Engineering Mechanics, University of Nebraska, Lincoln, NE* 68588-0526*, USA*)

([2] *Department of Chemistry, Medical Technology, and Physics, Monmouth University, West Long Branch, NJ* 07764-1898*, USA*)

([3] *Piezoelectric Device Laboratory, School of Mechanical Engineering and Mechanics, Ningbo University, Ningbo* 315211*, China*)

Received 1 June 2011, revision received 7 May 2012

ABSTRACT We study free vibration of a thickness-shear mode crystal resonator of AT-cut quartz. The resonator is a rectangular plate partially and symmetrically electroded at the center with rectangular electrodes. A single-mode, three-dimensional equation governing the thickness-shear displacement is used. A Fourier series solution is obtained. Numerical results calculated from the series show that there exist trapped thickness-shear modes whose vibration is mainly under the electrodes and decays rapidly outside the electrodes. The effects of the electrode size and thickness on the trapped modes are examined.

KEY WORDS crystal, wave, vibration, plate, three-dimensional effect

I. INTRODUCTION

Piezoelectric crystals are widely used to make acoustic wave resonators as a frequency standard for time-keeping, frequency generation and operation, telecommunication, and sensing. Quartz is the most widely used crystal for resonators. A large portion of quartz resonators operate with the so-called thickness-shear (TSh) modes of a plate[1,2]. Theoretically, pure TSh modes can only exist in unbounded plates without edge effects, and the plates have to be either completely unelectroded or totally electroded. When a plate is vibrating in TSh modes, motions of the material particles of the plate are parallel to the plate surfaces. The velocities of the particles of the plate vary along the plate thickness only, without in-plane variations. TSh modes are the ideal operating modes of crystal resonators and many other acoustic wave devices.

In real devices, however, finite crystal plates are used for which pure TSh modes cannot exist because of edge effects. In addition, crystal plates partially electroded at the center called trapped energy resonators are often used to achieve energy trapping with which the TSh vibration is essentially confined under the electrodes and decays outside the electrodes. Therefore, in real devices, due to the edges of finite plates and/or partial electrodes, the actual operating TSh modes in fact have slow in-plane variations and are called transversely varying TSh modes[3]. Since resonators are made smaller

* Corresponding author. E-mail: wangji@nbu.edu.cn

** Project supported by the National Natural Science Foundation of China (No. 10932004), the Doctoral Program Fund of the Ministry of Education of China (No. 20093305110003), the K. C. Wong Magna Fund of Ningbo University and the U.S. Army Research Office (No. W911NF-10-1-0293).

and smaller for miniaturization, edge effects and energy trapping have become more crucial. There is a growing need for better understanding and more accurate prediction of transversely varying TSh modes with in-plane variations.

Due to the anisotropy of crystals, analyzing crystal resonators using the three-dimensional (3-D) theory of elasticity or piezoelectricity presents considerable mathematical challenges. Usually various approximations need to be made. Two approaches are often used. One is to develop approximate, two-dimensional (2-D) plate equations[4–6] to simplify the problems so that theoretical analyses are possible. The other is to use numerical techniques like the finite element method. There exist numerous theoretical results from the 2-D plate equations for TSh modes (see the references in Ref.[7], a review article). Most of the results in Ref.[7] are for strip resonators with in-plane variation in one direction only. For rectangular plate resonators with modes varying in both of the in-plane directions, existing theoretical analyses are relatively few and are based on 2-D plate theories[8–12]. When using plate equations to analyze partially electroded plates, equations and solutions for the electroded and unelectroded regions have to be obtained separately and then joined by continuity conditions among the electroded and unelectroded regions. This is very complicated and sometimes impractical or even impossible.

In this paper we study energy trapping of TSh modes in a partially electroded rectangular quartz resonator. This problem is fundamental to energy trapping in resonators and is challenging when analyzed by 2-D plate equations. We propose using the 3-D equations of anisotropic elasticity with Fourier series. This approach can handle the piecewise boundary conditions associated with the partial electrodes and the unelectroded areas at the plate top and bottom surfaces effectively in a global manner, without the need of dividing the plate into electroded and unelectroded regions. Thus the problem can be solved and computed efficiently. This allows us to examine how the resonant frequencies, mode shapes, and energy trapping are affected by the electrode mass and dimension. These data are important in resonator design and optimization.

II. GOVERNING EQUATIONS

Consider an AT-cut quartz plate as shown in Fig.1. x_2 is the plate normal. x_1 and x_3 are the in-plane coordinates. The general 3-D equations of motion and electrostatics for an AT-cut quartz plate as a piezoelectric crystal in terms of the displacement vector u_i and the electric potential ϕ can be found in Ref.[13,14]. These equations are lengthy and are rarely used in their original form to analyze a problem, and therefore are not provided here. Quartz is a material with very weak piezoelectric coupling. For a free vibration frequency analysis, we will neglect the small piezoelectric coupling as usual and perform an elastic analysis. Following[15], we also neglect the relatively small elastic constants c_{14}, c_{24} and c_{56}. In finite plate TSh resonators, the operating TSh mode u_1 may be coupled to other undesirable modes. The main coupling is with the plate flexural mode described by u_2. Therefore we also neglect the less coupled displacement u_3 and drop the equation of motion for u_3 accordingly Ref.[15]. With the above common approximations in the analysis of quartz devices, the remaining displacement equations of motion are

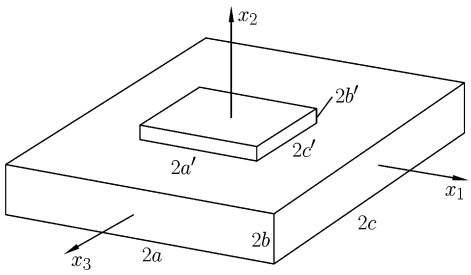

Fig. 1 A rectangular plate of rotated Y-cut quartz with a pair of symmetric, partial electrodes.

$$\begin{aligned} &c_{11}u_{1,11}+(c_{12}+c_{66})u_{2,12}+c_{66}u_{1,22}+c_{55}u_{1,33}=\rho\ddot{u}_1\\ &(c_{66}+c_{12})u_{1,12}+c_{66}u_{2,11}+c_{22}u_{2,22}+c_{44}u_{2,33}=\rho\ddot{u}_2 \end{aligned} \tag{1}$$

and the corresponding constitutive relations for stress components in terms of the displacement gradients become

$$\begin{aligned} &T_{11}=c_{11}u_{1,1}+c_{12}u_{2,2}, \quad T_{22}=c_{12}u_{1,1}+c_{22}u_{2,2}, \quad T_{33}=c_{13}u_{1,1}+c_{23}u_{2,2}+c_{34}u_{2,3}\\ &T_{23}=c_{44}u_{2,3}, \quad T_{31}=c_{55}u_{1,3}, \quad T_{12}=c_{66}(u_{1,2}+u_{2,1}) \end{aligned} \tag{2}$$

Equations (1) and (2) are essentially the same as Eq.(1.7) of Ref.[15] when the small piezoelectric coupling is neglected. The only difference is that Eq.$(1)_2$ has a term related to c_{44} which was neglected in Ref.[15] and we keep it here for the sake of entirety of equations until its elimination later. Equation (1) is for coupled TSh u_1 and flexure u_2. The coupling between TSh and flexure in a plate has been

thoroughly studied and well understood[16–22]. It depends on the plate dimensions and is strong only for certain aspect ratios (length/thickness) of the plate. For thin plates with a large aspect ratio it is less likely to happen. For our purpose, it is sufficient to assume that the coupling to flexure has been avoided through proper design of the plate dimensions. Therefore we further neglect the flexural displacement u_2 and consider transversely varying TSh modes with one displacement component $u_1(x_1, x_2, x_3, t)$ only. In this case Eqs.(1) and (2) are reduced to

$$c_{11}u_{1,11} + c_{66}u_{1,22} + c_{55}u_{1,33} = \rho\ddot{u}_1 \tag{3}$$

$$\begin{array}{lll} T_{11} = c_{11}u_{1,1}, & T_{22} = c_{12}u_{1,1}, & T_{33} = c_{13}u_{1,1} \\ T_{23} = 0, & T_{31} = c_{55}u_{1,3} & T_{12} = c_{66}u_{1,2} \end{array} \tag{4}$$

Equation (3) is the same as Eq.(2) of Ref.[23]. It was also used in Ref.[24]. When a plate is vibrating in transversely varying TSh modes, $u_{1,2}$ is the major term. Derivatives with respect to the in-plane coordinates x_1 and x_3 are small for slow in-plane variations.

The plate in Fig.1 is partially electroded in the central region. The electrodes at the plate top and bottom are identical and symmetric. They are assumed to be very thin and only their inertia will be considered. Their stiffness will be neglected. The boundary conditions at the plate top and bottom are

$$T_{21} = \begin{cases} \mp 2\rho' b' \ddot{u}_1 & (x_2 = \pm b, \quad |x_1| < a', \quad |x_3| < c') \\ 0 & (x_2 = \pm b, \quad \text{elsewhere}) \end{cases} \tag{5}$$

In the electroded areas, the boundary condition in Eq.(5) represents Newton's second law applied to the electrodes. Corresponding to Eq.(3), the traction-free boundary conditions at the plate edges are[15, 25]

$$\begin{array}{ll} T_{12} = 0 & (x_1 = \pm a, \quad |x_2| < b, \quad |x_3| < c) \\ T_{31} = 0 & (x_3 = \pm c, \quad |x_2| < b, \quad |x_1| < a) \end{array} \tag{6}$$

III. UNELECTRODED PLATE

We consider a special case first. Let the plate be unelectroded[24]. In this case $a' = c' = 0$. For resonator applications we are interested in modes antisymmetric in x_2 and symmetric in x_1 and x_3. Therefore we try the following fields[25]:

$$u_1 = A \sin\frac{l\pi x_2}{2b} \cos\frac{m\pi x_1}{2a} \cos\frac{n\pi x_3}{2c} \exp(\mathrm{i}\omega t) \tag{7}$$

where

$$l = 1, 3, 5, \cdots, \quad m = 1, 3, 5, \cdots, \quad n = 0, 2, 4, \cdots \tag{8}$$

m and n assume odd and even integers, respectively as the boundary conditions are effectively $u_1 = 0$ at $x_1 = \pm a$ and $u_{1,3} = 0$ at $x_3 = \pm c$, respectively, according to Eqs.(6) and (4). In Ref.[25] there are three other sets of modes for which at least one dependent on x_1 or x_3 is odd and therefore those modes are not of interest. Equation (7) can be obtained by the standard procedure of separation of variables. It satisfies all of the traction-free boundary conditions in Eqs.(5) and (6). Substitution of Eq.(7) into Eq.(3) determines the resonant frequencies as

$$\rho\omega_{lmn}^2 = c_{66}\left(\frac{l\pi}{2b}\right)^2 + c_{11}\left(\frac{m\pi}{2a}\right)^2 + c_{55}\left(\frac{n\pi}{2c}\right)^2 \tag{9}$$

Equation (9) is the same as Eq.(7.17) of Ref.[24]. It can be further written as

$$\frac{\omega_{lmn}^2}{\omega_s^2} = l^2 + \frac{c_{11}}{c_{66}}\left(m\frac{b}{a}\right)^2 + \frac{c_{55}}{c_{66}}\left(n\frac{b}{c}\right)^2 \tag{10}$$

where

$$\omega_s = \frac{\pi}{2b}\sqrt{\frac{c_{66}}{\rho}} \tag{11}$$

ω_s is the resonant frequency of the fundamental TSh mode in an unbounded quartz plate without electrodes.

IV. FULLY ELECTRODED PLATE

Next we consider another special case in which the crystal plate is fully electroded, i.e., $a' = a$ and $c' = c$. We consider the possibility of the following fields:

$$u_1 = A\sin(\eta_{mn}x_2)\cos\frac{m\pi x_1}{2a}\cos\frac{n\pi x_3}{2c}\exp(\mathrm{i}\omega t) \tag{12}$$

Equation (12) satisfies the edge conditions in Eq.(6). For Eq.(12) to satisfy Eq.(3), we must have

$$\eta_{mn}^2 = \frac{1}{c_{66}}\left[\rho\,\omega^2 - c_{11}\left(\frac{m\pi}{2a}\right)^2 - c_{55}\left(\frac{n\pi}{2c}\right)^2\right] \tag{13}$$

Quartz resonators are made from thin plates with large a and c ($a, c >> b$). In this case, for m and n that are not large, η_{mn}^2 is positive. We are interested in the first few TSh modes with no more than a couple of nodal points along the x_1 and x_3 directions described by a small m or n. In this case η_{mn}^2 is positive. Substitution of Eq.(12) into the plate top and bottom boundary conditions in Eq.(5) gives

$$\cot(\eta_{mn}b) = \frac{\pi^2}{4}\frac{R}{\eta_{mn}b}\frac{\omega^2}{\omega_s^2} \quad (m = 1, 3, 5, \cdots, \quad n = 0, 2, 4, \cdots) \tag{14}$$

where

$$R = \frac{2\rho' b'}{\rho b} \tag{15}$$

R is the mass ratio between the electrodes and the crystal plate. We look for an approximate solution to Eq.(14) when the electrodes are thin and R is small. The lowest-order approximation when $R = 0$ is given by $\eta_{mn}b = l\pi/2$ or Eq.(10). For the next order of approximation we write

$$\eta_{mn}b = \frac{l\pi}{2} - \Delta_l \quad (l = 1, 3, 5, \cdots) \tag{16}$$

where Δ_l is small. Substituting Eq.(16) into Eq.(14), for small Δ_l and small R, we obtain

$$\Delta_l = \frac{\pi R}{2l}\left[l^2 + \frac{c_{11}}{c_{66}}\left(m\frac{b}{a}\right)^2 + \frac{c_{55}}{c_{66}}\left(n\frac{b}{c}\right)^2\right] \tag{17}$$

Substitution of Eq.(17) into Eq.(16), with the use of Eq.(13), yields approximately,

$$\frac{\omega_{lmn}^2}{\omega_s^2} = (1 - 2R)\left[l^2 + \frac{c_{11}}{c_{66}}\left(m\frac{b}{a}\right)^2 + \frac{c_{55}}{c_{66}}\left(n\frac{b}{c}\right)^2\right] \tag{18}$$

Equation (18) shows that the electrode inertia lowers the frequencies. When $R = 0$, Eq.(18) is reduced to Eq.(10).

V. PARTIALLY ELECTRODED PLATE

Now we go back to the general situation of a partially electroded quartz plate. In this case, a single mode like Eq.(7) or (12) is insufficient and a series representation of the displacement field is needed.

5.1. Fourier Series Solution

We construct the following series solution:

$$u_1 = \sum_{m,n} A_{mn}\sin(\eta_{mn}x_2)\cos\frac{m\pi x_1}{2a}\cos\frac{n\pi x_3}{2c}\exp(\mathrm{i}\omega t) \tag{19}$$

where $m = 1, 3, 5, \cdots$, $n = 0, 2, 4, \cdots$, A_{mn} are undetermined constants, and η_{mn} is still given by Eq.(13). Equation (19) satisfies Eqs.(3) and (6). To apply the boundary conditions at the plate top and bottom in Eq.(5), from Eq.(19) we calculate

$$T_{21} = c_{66}u_{1,2} = \sum_{m,n} c_{66}\eta_{mn}A_{mn}\cos(\eta_{mn}x_2)\cos\frac{m\pi x_1}{2a}\cos\frac{n\pi x_3}{2c}\exp(\mathrm{i}\omega t) \tag{20}$$

Substitution of Eqs.(19) and (20) into Eq.(5) gives

$$\sum_{m,n} c_{66}\eta_{mn}A_{mn}\cos(\eta_{mn}b)\cos\frac{m\pi x_1}{2a}\cos\frac{n\pi x_3}{2c} = \begin{cases} 2\rho' b'\omega^2\sum\limits_{m,n} A_{mn}\sin(\eta_{mn}b)\cos\dfrac{m\pi x_1}{2a}\cos\dfrac{n\pi x_3}{2c} & (|x_1|<a', \quad |x_3|<c') \\ 0 & \text{(elsewhere)} \end{cases} \tag{21}$$

Due to the antisymmetry about $x_2 = 0$, the boundary conditions at $x_2 = \pm b$ lead to the same equation as in Eq.(21). We multiply both sides of Eq.(21) by $\cos[p\pi x_1/(2a)]\cos[q\pi x_3/(2c)]$ with $p = 1, 3, 5, \cdots$ and $q = 0, 2, 4, \cdots$, and integrate the resulting expression over the area of $|x_1| < a$, $|x_3| < c$ to obtain

$$c_{66}\eta_{mn}A_{mn}\cos(\eta_{mn}b)\int_{-a}^{a}\cos^2\frac{p\pi x_1}{2a}\mathrm{d}x_1\int_{-c}^{c}\cos^2\frac{q\pi x_3}{2c}\mathrm{d}x_3 = 2\rho' b'\omega^2\sum_{m,n}A_{mn}\sin(\eta_{mn}b)C_{mp}D_{nq} \qquad (m,p=1,3,5\cdots, \quad n,q=0,2,4,\cdots) \tag{22}$$

where we have denoted

$$C_{mp} = \int_{-a'}^{a'}\cos\frac{m\pi x_1}{2a}\cos\frac{p\pi x_1}{2a}\mathrm{d}x_1 = C_{pm} \qquad (m,p=1,3,5,\cdots)$$
$$D_{nq} = \int_{-c'}^{c'}\cos\frac{n\pi x_3}{2c}\cos\frac{q\pi x_3}{2c}\mathrm{d}x_3 = D_{qn} \qquad (n,q=0,2,4,\cdots) \tag{23}$$

Equation (23) is a system of linear homogeneous equations for A_{mn}. For nontrivial solutions the determinant of the coefficient matrix has to vanish, which determines the resonant frequencies together with Eq.(13). The nontrivial solutions of A_{mn} determine the corresponding modes. This is a complicated eigenvalue problem since the eigenvalue or the resonant frequency is present in every η_{mn}.

5.2. Numerical Results

We introduce

$$\bar{\omega}_s = \omega_s(1-R) \tag{24}$$

$\bar{\omega}_s$ is the resonant frequency of the fundamental TSh mode in an unbounded, fully electroded quartz plate. The resonant frequencies of the modes we are interested in are within $\bar{\omega}_s < \omega < \omega_s$.

Consider a resonator with $2a = 12.5$ mm, $2a' = 7.5$ mm, $2c = 10$ mm, $2c' = 5$ mm and $2b = 0.25$ mm. The mass ratio $R = 3\%$. Five frequencies, $\omega_1 = 4.049652\times10^7$ rad/s, $\omega_2 = 4.0725961\times10^7$ rad/s, $\omega_3 = 4.113085\times10^7$ rad/s, $\omega_4 = 4.134699\times10^7$ rad/s and $\omega_5 = 4.154118\times10^7$ rad/s, are found in $\bar{\omega}_s < \omega < \omega_s$. When using eight terms in the series for both of the x_1 and x_3 directions, the five frequencies are the same as those obtained using nine terms in both of the x_1 and x_3 directions within six significant figures. Therefore eight terms are used in each direction for the numerical results below. The total number of terms in the series is sixty-four.

Figure 2 shows the five modes in the order of increasing frequency. For all of them the vibration is large in the central region and small near the plate edges. In other words the vibration is mainly under the electrodes and decays outside them. This is the so-called energy trapping by electrodes. Energy trapping is crucial to device mounting. For trapped modes, mounting can be done near the plate edges without affecting the vibration of the plate. In the first mode, the whole plate is vibrating in phase. In the second mode and the third mode, there is a nodal line. In such a case the charges on an electrode produced by the shear strain tend to cancel each other and thus reduce the capacitance of the resonator. This may be undesirable or desirable depending on the specific application. For higher order modes there are more nodal lines.

Figure 3 shows the effect of the electrode dimension on energy trapping in both of the x_1 and x_3 directions. Numerical results show that smaller electrodes are associated with fewer trapped modes with higher frequencies. It can be seen in Fig.3 that in general the vibration distribution follows the electrodes. For smaller electrodes the vibration is more trapped near the center. The behaviors of the

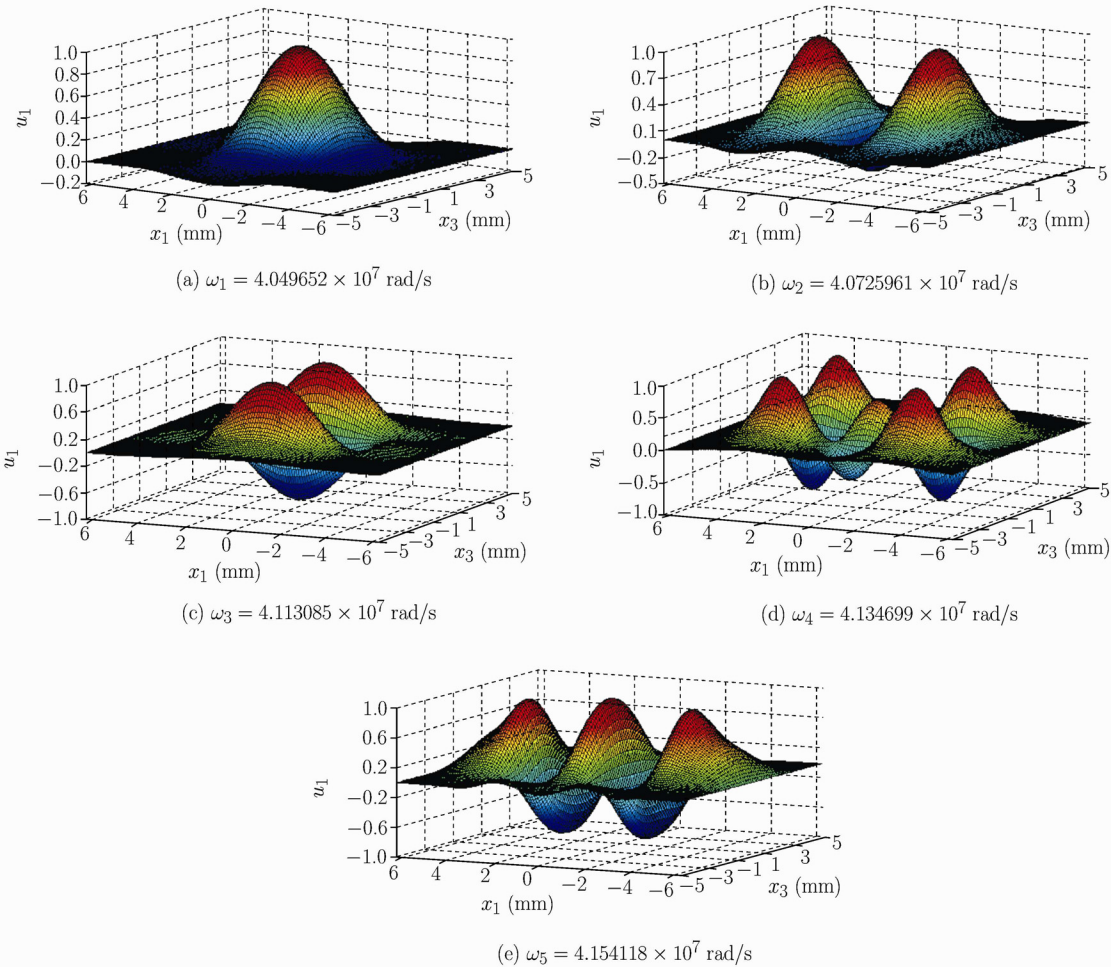

(a) $\omega_1 = 4.049652 \times 10^7$ rad/s

(b) $\omega_2 = 4.0725961 \times 10^7$ rad/s

(c) $\omega_3 = 4.113085 \times 10^7$ rad/s

(d) $\omega_4 = 4.134699 \times 10^7$ rad/s

(e) $\omega_5 = 4.154118 \times 10^7$ rad/s

Fig. 2. Five frequencies of trapped modes with $2a$=12.5 mm, $2a'$=7.5 mm, $2c$=10 mm, $2c'$=5 mm, and $2b$=0.25 mm.

modes near the edges are different in the x_1 and x_3 directions. According to the boundary conditions, at $x_1 = \pm a$ we have $u_1 = 0$ and at $x_3 = \pm c$ we have $u_{1,3} = 0$. Therefore in Fig.3(a) we have vanishing u_1 at the edges while in Fig.3(b) the modes are essentially flat near the edges. In Fig.3(a), for the case of large electrodes, the mode has no nodal points (zeros). For the two cases of small and medium electrodes, the modes have nodal points. For small electrodes the nodal points are outside the electrodes and thus will not cause charge cancellation on the electrodes. For medium electrodes the nodal points are within the electrodes and are near the electrode edges, which causes small charge cancellations. In Fig.3 (b), the modes corresponding to large electrodes have nodal points under the electrodes which are near the electrode edges. The case of medium electrodes has nodal points outside the electrodes. For the case of small electrodes represented by the solid line in Fig.3(b), both $u_{1,3}$ and u_1 are small near the edges which is ideal.

Figure 4 shows the effect of the mass ratio R on the first mode. Again the behaviors in the x_1 and x_3 directions are different. The frequency of the first mode decreases as R increases, as expected. Numerical results show that larger values of R increase the number of trapped modes. In general for larger values of R the mode is pushed further toward the center with better energy trapping. However, as the mode is pushed toward the center, nodal points tend to appear which cause charge cancellation on the electrodes unless the electrodes are shortened accordingly. Since both energy trapping and charge cancellation affect the motional capacitance of the resonator, how to maximize the capacitance requires careful design with the necessity of considering both the electrode size and thickness, as well as different behaviors along x_1 and x_3.

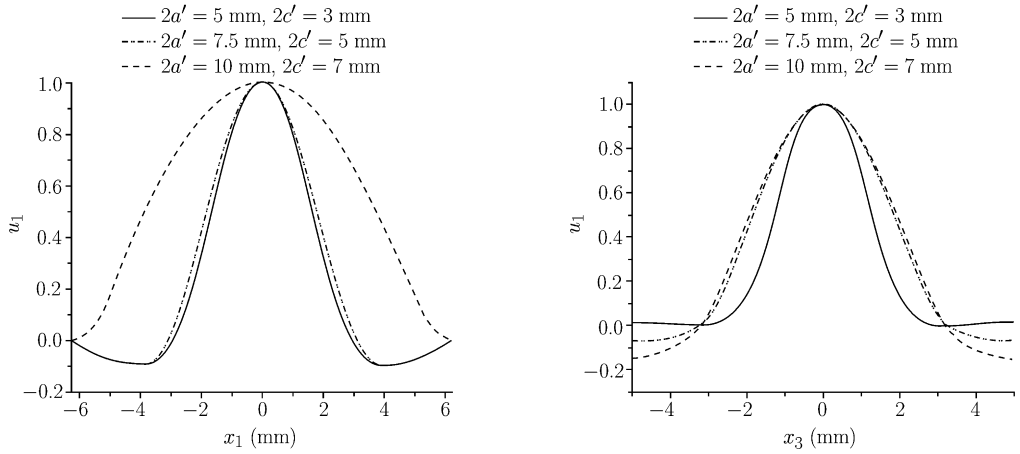

(a) Variation along x_1 (b) Variation along x_3

Fig. 3. Effect of electrode size on the first energy trapping mode with R=3%. ($2a'$=5 mm, $2c'$=3 mm: 2 trapped modes with $\omega_1 = 4.070822 \times 10^7$ rad/s; $2a' = 7.5$ mm, $2c' = 5$ mm: 5 trapped modes with $\omega_1 = 4.049652 \times 10^7$ rad/s; $2a' = 10$ mm, $2c' = 7$ mm: 7 trapped modes with $\omega_1 = 4.023059 \times 10^7$ rad/s).

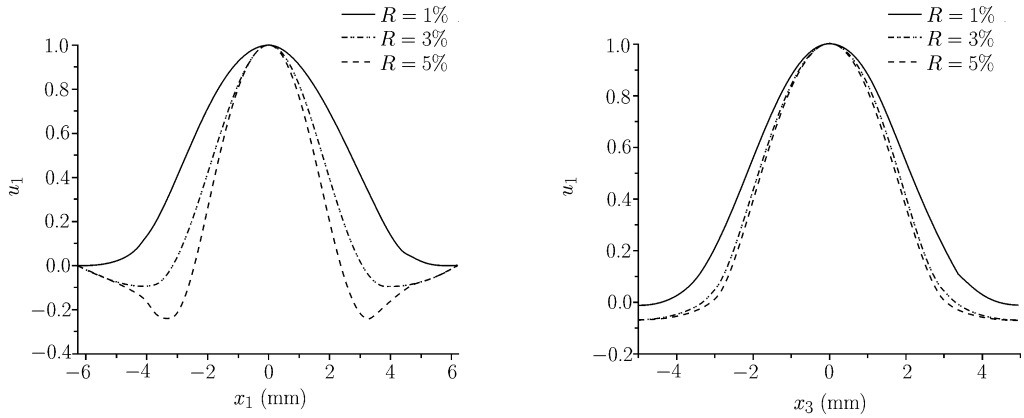

(a) Variation along x_1 (b) Variation along x_3

Fig. 4. Effect of electrode thickness on energy trapping. ($2a'$=7.5 mm, $2c'$=5 mm. R=1%: 2 trapped modes with $\omega_1 = 4.130107 \times 10^7$ rad/s; $R = 3\%$: 5 trapped modes with $\omega_1 = 4.049652 \times 10^7$ rad/s; $R = 5\%$: 7 trapped modes with $\omega_1 = 3.966399 \times 10^7$ rad/s).

VI. CONCLUSION

The simplified equation for u_1 only and the Fourier series solution obtained are able to show some basic behaviors of a partially electroded quartz plate TSh resonator. Partial electrodes at the central portion of a plate can produce energy trapping of TSh modes. The trapped modes are sensitive to the electrode inertia and dimensions. Typically there exist a few trapped modes near the fundamental TSh frequency. Larger and thicker electrodes lower the resonant frequencies and trap more modes. The behaviors of energy trapping in the x_1 and x_3 directions are different due to the difference in the corresponding boundary conditions. Varying the electrode dimension or thickness can also affect the existence and the locations of the nodal points of the first mode which may lead to charge cancellation on the electrodes and affect the capacitance of the resonator. The method presented with focus on the thickness-shear mode can also be applied to the same modes in other materials for acoustic wave resonators.

References

[1] Koga,I., Thickness vibrations of piezoelectric oscillating crystals. *Physics*, 1932, 3: 70-80.

[2] Tiersten,H.F., Thickness vibrations of piezoelectric plates. *The Journal of the Acoustical Society of America*, 1963, 35: 53-58.
[3] Tiersten,H.F., A corrected modal representation of thickness vibrations in quartz plates and its influence on the transversely varying case. *IEEE Transactions on Ultrasonics, Ferroelectrics, and Frequency Control*, 2003, 50: 1436-1443.
[4] Tiersten,H.F. and Mindlin,R.D., Forced vibrations of piezoelectric crystal plates. *Quarterly of Applied Mathematics*, 1962, 20: 107-119.
[5] Mindlin,R.D., High frequency vibrations of piezoelectric crystal plates. *International Journal of Solids Structures*, 1972, 8: 895-906.
[6] Lee,P.C.Y., Syngellakis,S. and Hou,J.P., A two-dimensional theory for high-frequency vibrations of piezoelectric crystal plates with or without electrodes. *Journal of Applied Physics*, 1987, 61: 1249-1262.
[7] Wang,J. and Yang,J.S., Higher-order theories of piezoelectric plates and applications. *Applied Mechanics Reviews*, 2000, 53: 87-99.
[8] Mindlin,R.D. and Deresiewicz,H., Thickness-shear and flexural vibration of rectangular crystal plates, *Journal of Applied Physics*, 1955, 26: 1435-1442.
[9] Lee,P.C.Y. and Spencer,W.J., Shear-flexure-twist vibrations in rectangular AT-cut quartz plates with partial electrodes. *The Journal of the Acoustical Society of America*, 1969, 45: 637-645.
[10] Lee,P.C.Y. and Chen,S.S., Vibrations of contoured and partially plated, contoured, rectangular, AT-cut quartz plates. *The Journal of the Acoustical Society of America*, 1969, 46: 1193-1202.
[11] Mindlin,R.D. and Gazis,D.C., Srong resonances of rectangular AT-cut quartz plates. *Proceedings of the Fourth U.S. National Congress of Applied Mechanics*, 1962, 305-310.
[12] Zhang,C.L., Chen,W.Q. and Yang,J.S., Electrically forced vibration of a rectangular piezoelectric plate of monoclinic crystals. *International Journal of Applied Electromagnetics and mechanics*, 2009, 31: 207-218.
[13] Tiersten,H.F., Linear Piezoelectric Plate Vibrations. New York: Plenum, 1969.
[14] Meitzler,A.H., Berlincourt D., Welsh,F.S.,III, Tiersten,H.F., Coquin,G.A. and Warner,A.W., IEEE Standard on Piezoelectricity. IEEE, New York, 1988.
[15] Tiersten,H.F., Analysis of trapped-energy resonators operating in overtones of coupled thickness shear and thickness twist. *The Journal of the Acoustical Society of America*, 1976, 59: 879-888.
[16] Mindlin,R.D., Thickness-shear and flexural vibrations of crystal plates. *Journal of Applied Physics*, 1951, 22: 316-323.
[17] Mindlin,R.D., Forced thickness-shear and flexural vibrations of piezoelectric crystal plates. *Journal of Applied Physics*, 1952, 23: 83-88.
[18] Mindlin,R.D. and Lee,P.C.Y., Thickness-shear and flexural vibrations of partially plated, crystal plates. *International Journal of Solids Structures*, 1966, 2: 125-139.
[19] Shen,F., Lee,K.H., O'Shea,S.J., Lu,P. and Ng,T.Y., Frequency interference between two quartz crystal microbalances. *IEEE Sensors Journal*, 2003, 3: 274-281.
[20] Shen,F. and Lu,P., Influence of interchannel spacing on the dynamical properties of multichannel quartz crystal microbalance. *IEEE Transactions on Ultrasonics, Ferroelectrics, and Frequency Control*, 2003, 50: 668-675.
[21] Wang,J. and Zhao,W.H., The determination of the optimal length of crystal blanks in quartz crystal resonators. *IEEE Transactions on Ultrasonics, Ferroelectrics, and Frequency Control*, 2005, 52: 2023-2030.
[22] Wang,J., Zhao,W.H. and Du,J.K., The determination of electrical parameters of quartz crystal resonators with the consideration of dissipation. *Ultrasonics*, 2006, 44: E869-E873.
[23] Wilson,C.J., Vibration modes of AT-cut convex quartz resonators. *Journal of Physics D: Applied Physics*, 1974, 7: 2449-2454.
[24] McSkimin,H.J., Theoretical analysis of modes of vibration for isotropic rectangular plates having all surfaces free. *Bell System Technical Journal*, 1944, 23: 151-177.
[25] Tiersten,H.F. and Smyth,R.C., Coupled thickness-shear and thickness-twist vibrations of unelectroded AT-cut quartz plates. *The Journal of the Acoustical Society of America*, 1985, 78: 1684-1689.